AIP Advances

Taking internally wetted capillary electrospray emitters to the sub-ten-micrometer scale with 3D microlithography

Cite as: AIP Advances **11**, 105315 (2021); https://doi.org/10.1063/5.0066619
Submitted: 06 September 2021 • Accepted: 20 September 2021 • Published Online: 08 October 2021

Fynn L. Kunze, Torsten Henning and Peter J. Klar

Taking internally wetted capillary electrospray emitters to the sub-ten-micrometer scale with 3D microlithography

Cite as: AIP Advances 11, 105315 (2021); doi: 10.1063/5.0066619
Submitted: 6 September 2021 • Accepted: 20 September 2021 •
Published Online: 8 October 2021

Fynn L. Kunze,[a] Torsten Henning, and Peter J. Klar

AFFILIATIONS

Institute of Experimental Physics I and Center for Materials Research ZfM/LaMa, Justus Liebig University, Heinrich-Buff-Ring 16, DE-35392 Giessen, Germany

[a]Author to whom correspondence should be addressed: Fynn.Kunze@physik.uni-giessen.de

ABSTRACT

Electrospray emitters are an obvious choice for miniaturized thrusters for a variety of applications on small satellites (e. g., CubeSats), as well as for other micropropulsion purposes. They are inherently small and require a relatively low electric power for operation, and therefore, they fulfill the requirements imposed due to the small volume of CubeSats. Electrospray emitters of the internally wetted capillary type were fabricated by 3D microlithography in the SU-8 photopolymer down to capillary diameters of about 10 μm. Thus, the emitters are an order of magnitude smaller in lateral dimensions than those fabricated by advanced 3D printing methods and still half an order of magnitude smaller than those made by planar photolithography in SU-8. Fabrication methods and process parameters are presented. Furthermore, the preliminary results of the electric characterization of the emission behavior are shown. The experiments show promising results regarding the fabrication quality and extraction behavior.

I. INTRODUCTION AND MOTIVATION

In recent years, small satellites have become more and more important for both commercial and scientific purposes.[1–3] Alongside the demand for small satellites, the need for specialized micropropulsion systems arises. Specifically, electric propulsion systems have become more important due to their high efficiency and high specific impulse, resulting in good fuel and power economy, for purposes such as attitude and orbit control (AOC).[4–8]

There are two ways to develop miniaturized electric thruster systems for small satellites. The first is to scale down established thrusters, such as plasma-based propulsion systems, while the second is to develop systems from inherently small components. Electrospray emitters fall under the second approach to miniaturization, as they are inherently small and well suited for small satellites due to their low power requirements.[9]

These emitters utilize a static electric field applied between a liquid ion source (LIS) and an extraction electrode to extract droplets or, ideally, single ions from the LIS. The liquid propellant is supplied to an extraction site on the emitter surface, typically an orifice, where the liquid is exposed to the electric field. Under the influence of the (external) electric forces and the internal forces (cohesion) of the liquid, its meniscus is deformed, resulting in a cone-like shape, the so-called "Taylor cone."[10] At the tip of the cone, the electric forces are stronger than the internal hydraulic forces, thus allowing droplets or single ions to overcome the surface tension and form an ion spray, the so-called electrospray. The extracted ions can be further accelerated with suitable ion optics to generate thrust for small spacecraft.[11–13]

There are three basic emitter configuration types, namely, externally wetted emitters, porous emitters, and internally wetted capillary emitters that this paper focuses on. The three of them differ in the way the propellant is supplied to the extraction sites, while all three from there on follow the same operating principle described above.[14]

The hydraulic resistance of the propellant feed system has been identified as a key parameter for stable operation of the emitters.[15] A sufficiently high hydraulic resistance can only be achieved by the fabrication of structures with a high aspect ratio (length-to-diameter ratio), which is a difficult task in any field of microfabrication.

Porous emitters have an advantage in this respect because the fluidic path through the pores provides a high hydraulic resistance at the expense of introducing an element of randomness into the design and of imposing a lower size limit on the miniaturization of the individual emitter.

Porous emitters with liquid metal as a propellant (field emission electric propulsion or FEEP thrusters) are already in use on spacecraft and have flight heritage;[16,17] however, with the recent advances in microfabrication technologies, both in 3D printing and in silicon technologies, internally wetted capillary emitters appear to have become viable for thruster applications again. 3D printing techniques, such as vat printing [stereo-lithography apparatus/digital light processing (SLA/DLP) printing], and, for smaller critical lateral dimensions, two-photon laser lithography are new fabrication technologies that offer a high degree of freedom of design for electrospray emitters[18,19] and thus the possibility of re-addressing the subject of hydraulic resistance in miniaturized emitters. Moreover, the capability of 3D microlithography to create capillaries with diameters as small as single digit micrometer figures implies that emitters thus created are at least an order of magnitude smaller in lateral dimensions than internally wetted capillary type microemitters made by other advanced 3D printing methods reported in the literature and still about half an order of magnitude smaller than the emitters fabricated in SU-8 by planar lithography previously reported by the authors.[11,20,21]

The research aim of the authors is to create single internally wetted capillary microemitters with a footprint of less than 0.1×0.1 mm^2 and a well-defined (that is, involving no elements of randomness) geometry at the sub-micrometer level, with capillary diameters of 10 μm and below, that is, at a scale which roughly equals the typical pore size of porous emitters.

From such individual microemitters, arrays of suitable sizes should be possible to build in order to achieve the required thrust range for a given application ("scaling-up by numbering-up"). The propellant of choice is an ionic liquid, namely, EMIM-BF4, for the time being. EMIM-BF4 is an ionic liquid often used for space applications. Technically, an ionic liquid is a salt with a very low melting point. Thus, it retains a liquid state at room temperature and below. Ionic liquids feature multiple advantages for space applications, such as negligible vapor pressure in vacuum environments, a high conductivity, and pre-ionization. EMIM-BF4 is composed of two molecules of similar molecular weight and opposite charges. EMIM (1-ethyl-3-methylimidazolium) is an organic molecule featuring a ring structure and a positive charge. BF4 (tetrafluoroborate) is an inorganic ion with a negative charge. Should the need arise, there are many different kinds of ionic liquids available, which would allow one to choose a suitable substitute for EMIM-BF4.[12,22]

II. MATERIALS AND METHODS

A. Fabrication methods and parameters

The fabrication method of choice for the essential parts of the microemitters is 3D microlithography in the form of two-photon lithography, realized in the commercial fabrication tool Photonic Professional GT (PPGT) from Nanoscribe (nanoscribe.com). The operating principle of the Nanoscribe PPGT is illustrated in Fig. 1. Light from a near-infrared fiber laser is focused through microscope optics. The single near-infrared photon does not carry enough

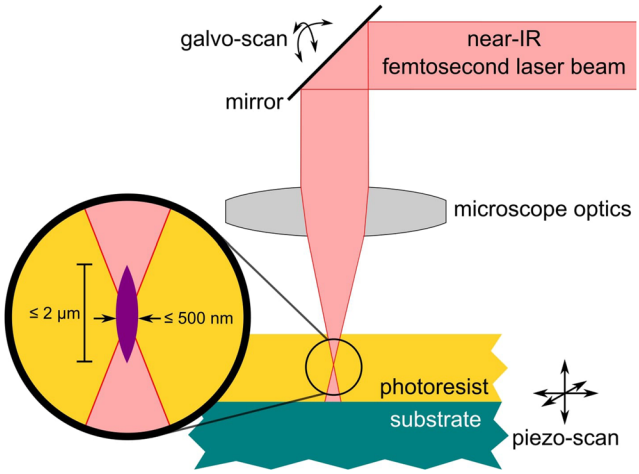

FIG. 1. Operating principle of two-photon lithography.

energy to trigger the photochemical reaction in the resist. However, in a small volume element (voxel) around the focus, the intensity is so high that two-photon processes occur. Two photons combined possess enough energy to start the photochemical reaction. The voxel typically has an extension of ~2 μm in the vertical direction and of less than the laser wavelength in lateral dimensions. By scanning this voxel through the resist, almost arbitrary shapes can be written. There are two scanning modes, namely, galvo scan, in which the laser beam is moved by galvo mirrors in the beam path, and piezo scan, in which the piezo stage carrying the sample is moved. Scanning in the vertical direction is always done in the piezo mode. Galvo scan offers an advantage in higher writing speed of about two orders of magnitude compared to piezo scan.

While there are resists optimized for use with the Nanoscribe PPGT, the authors opted to continue the use of SU-8 as a negative tone photostructurable epoxy polymer. Despite its most challenging properties for successful microfabrication, that is, the internal stress to which swelling during development is an important contribution, SU-8's superior resistance against harsh environments makes it a proven material for microfluidic applications.[23] One of the major beneficial properties of SU-8 is its chemical inertness. It is resistant to prolonged exposure to ionic liquids. Furthermore, currently, experiments under space-like conditions are conducted to verify if SU-8 is a suitable material for this application. SU-8 has a long heritage in high aspect ratio microlithography, and there is considerable knowledge regarding the optimization of the microlithography processes.[24]

3D lithography offers the possibility of creating undercut structures, which will become more important once the integration of the extraction electrodes or even more complex ion optics are considered.[25] At the present stage, the main objective of fabrication is to create well-defined single emitters with capillaries with a diameter as small as possible, integrated with a base plate with an edge length of a few millimeters that allows the handling of the emitter structure in the characterization setup. Mechanical stability and minimum warping of the base plate is a design target that needs to be

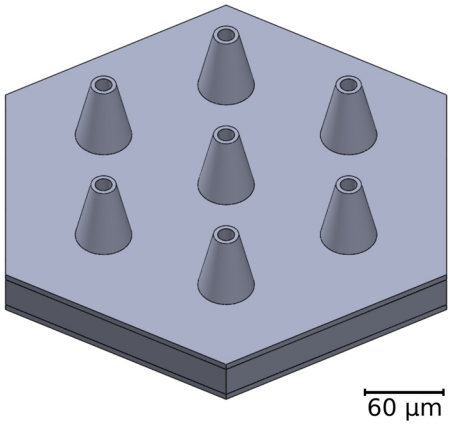

FIG. 2. 3D rendering of a CAD file defining an emitter array featuring seven individual volcano emitters and (a part of the) base plate.

traded-off against the requirement to keep writing times within reasonable bounds.

The basic shape of an individual emitter is that of a volcano.[26] One of the most important functions of the volcano shape is the mitigation of wetting of the area around the orifice by the ionic liquid.[20,21] Another benefit is the extension of the capillary's length and hence the hydraulic resistance without unduly extending the writing time. In addition, the volcano shape allows a good control of the electric field around the orifice and a strong enhancement of the electric field at that point. Figure 2 shows the CAD rendering of a small array of seven volcano microemitters on a base plate.

The volcano shape is not unique to emitters manufactured by two-photon lithography. Devices with lateral dimensions on the order of hundreds of micrometers made by 3D printing methods have been reported.[18,19]

The Nanoscribe PPGT works by writing lines. Areas are written by placing lines closed to each other (hatching). The optimum distance between lines (hatching distance) has to be determined by trading off the quality of writing against the writing time. Whether two neighboring hatching lines are written in the same direction or in opposite directions has been found to play no significant role in the projects presented here.

In the vertical (z) direction, subsequent layers are written at a fixed distance (slicing). As in hatching, the optimum slicing distance has to be determined as a compromise between the writing quality and time required. Since the structures to be written are larger than the areas that the galvo scan can cover in a single run, they have to be stitched together from the so-called chunks whose shape and arrangement are also subject to optimization. Careful chunking is critical for keeping the base plate warp as low as possible. Large volumes do not have to be written in their entirety. It is usually sufficient to write the outer surfaces and a number of support structures inside the volume. This technique is called "shell and scaffolding."

There are several routes to the set of line coordinates that are finally processed by the Nanoscribe PPGT:

- Sets of line coordinates can be produced by an external program and transferred as ASCII files.
- Lines can be algorithmically defined in the Nanoscribe-specific programming language (GWL files) that is interpreted by the NanoWrite software delivered with the instrument.
- The NanoWrite software can import standard 3D lithography CAD files, notably in the widespread STL format.

The latter approach is the most convenient one at the start of a project, and there are a number of options to control the behavior of the system in hatching, slicing, and chunking, but the control is nevertheless limited. Writing the GWL code allows for easy systematic variations of parameters and gives detailed control of the writing parameters for the most critical structures. Using an external programming language usually implies the generation of very large files that are inconvenient when rendering a visualization. In practice, a mix-and-match approach between CAD and import of STL files on the one hand and dedicated GWL code for the critical structures on the other hand has proven to be both convenient and economical. The typical process, design parameters for the volcano emitters, and writing parameters for the Nanoscribe PPGT system are listed in Table I.

The SU-8 resist (SU-8 50 from microchemicals.com) is spin-coated on a silicon wafer and pre-exposure-baked according to the manufacturer's specifications. To ensure good adhesion of the SU-8 to the wafer, an oxygen plasma cleaning of the wafer immediately before the coating is recommendable. When plasma cleaning is not available, a hydrofluoric acid dip of the wafer can be used instead.

When emitters are created by planar lithography, the silicon wafer acts as a sacrificial substrate, that is, it is removed at the end

TABLE I. Design parameters and process parameters for the fabrication of volcano emitters with the Nanoscribe PPGT 3D microlithography system.

Parameter	Value
Si wafer orientation	1-0-0
SU-8 resist thickness	≈130 μm
Surface offset	15 μm
Slicing distance	0.3 μm
Hatching distance	0.3 μm
Scanning speed, areas	100 000 μm s^{-1}
Scanning speed, details	50 000 μm s^{-1}
Relative laser power	35%
Base plate shape	Hexagonal
Base plate lateral size	5 × 5 mm^2
Base plate height	35 μm
Emitter height (height over base plate)	50 μm
Emitter diameter at base plate	(20 . . . 40) μm
Emitter diameter at top	(15 . . . 20) μm
Capillary diameter	(8 . . . 20) μm
Chunk shape	Honeycomb/hexagonal
Chunk side length	180 μm
Exposure time	≈12 h per complete unit
Post-exposure bake 65/95 °C	1/10 min
Development time	≈15 min

of the processing chain by wet chemical etching in warm potassium hydroxide solution. In this case, it is important that the wafer's surface orientation is 1-0-0, since a surface with that orientation can be attacked by the etchant.

In 3D microlithography with the resists optimized for this purpose, it is important to have a good contact between the written structure and the substrate. The writing process is therefore started at a certain distance below the substrate's surface as detected by the Nanoscribe system. This (negative) distance is known as the interface position. SU-8, however, turns out to be so viscous when processed as described above that the writing can actually be carried out entirely within the resist film at a fixed (surface) offset from the interface position. This implies that in the development step, the written structures are automatically detached from the substrate and that the wafer does no longer have to be dissolved. The wafer's surface orientation is then no longer important.

The post-exposure bake consists of two steps, first a hot plate bake for 60 s at 65 °C, then another bake for 10 min at 95 °C on a second hot plate. The samples are then developed in mr-Dev 600 (from www.microresist.de). Several developer baths may be used in series to minimize the risk of residues. Optionally, the development can be sped up by placing the beaker with the developer in a water bath with low power ultrasonic excitation. With the assistance of ultrasound, typical development times are on the order of 15 min. If "shell and scaffold" writing has been used, a flood exposure step has to be inserted in order to start the crosslinking of any resist remaining inside the shells. Flood exposure was carried out in a SUSS MA-56 mask aligner with a mercury high pressure vapor lamp (fly's eye not removed) and an exposure time of 10 s.

B. Characterization of the emission behavior

The experimental setup for the electrical characterization (both time-resolved and DC) is shown in Fig. 3. The emitter structures are glued to a PEEK holder with a two-component epoxy glue. At this stage, the quality of the glue connection and the continuity of the capillary are checked by filling the holder with deionized water and confirming under a microscope that a droplet occurs at the volcano tip only. Once the emitter has passed the quality check, the holder is mounted inside the vacuum chamber and connected to the propellant feed system. The propellant feed rate is controlled by a high precision infuse-withdrawal syringe pump (type KDS 900 OEM from www.kdscientific.com) with a mounted 25 μl syringe controlled by a computer. The ionic liquid is put at a high electric potential, whereas the annular shaped extraction electrode and the collector plate are grounded. The ion current impinging on the collector plate is passing a custom-built amplifier circuit whose output can be captured by digital multimeters for DC measurements and with an oscilloscope for time-resolved measurements. The cut-off frequency of the amplifier circuit is ~2 kHz due to the filter used. The custom-made electronics have the capability to resolve currents in the single nA range. No axial data can be acquired, such as the beam shape or the impact position on the detector plate, as the detector only features one collector plate.

III. RESULTS

A. Imaging of the emitter structures

The emitters fabricated as described above were characterized by scanning electron microscopy (SEM) and, in a destructive way, by milling with a focused ion beam (FIB) followed by SEM

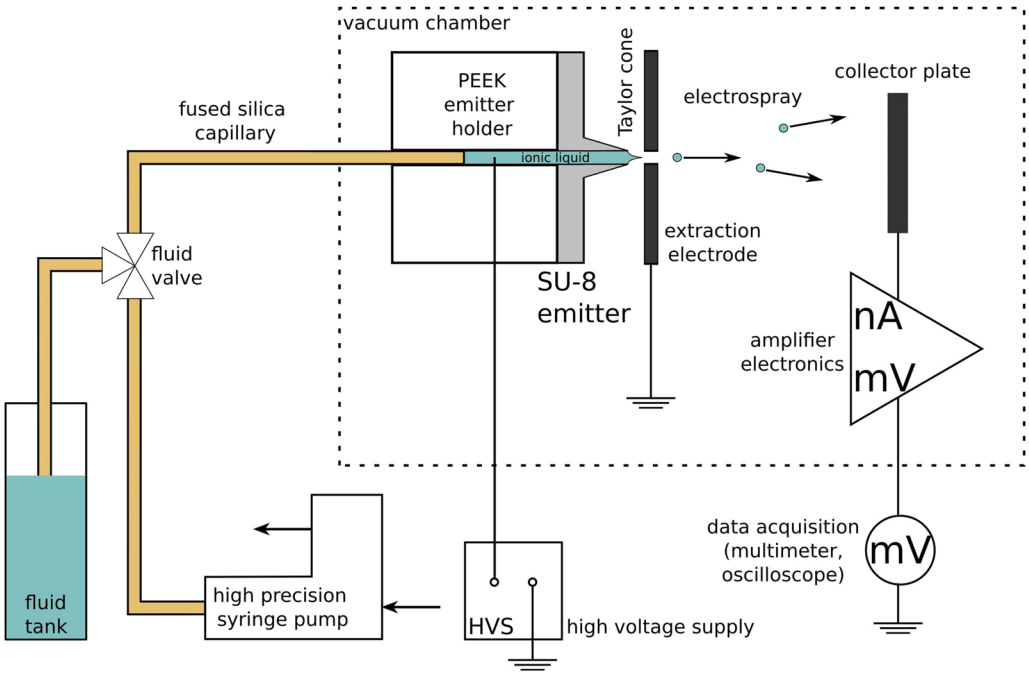

FIG. 3. Measurement setup for the characterization of the emission behavior.

inspection. Figure 4 shows two SEM images of a volcano emitter, taken at a slightly oblique angle from the top side (left panel) and from the back side (right panel).

The emitter has a height of 50 μm above the base plate whose thickness is 35 μm, and diameters of 35 and 16 μm at the base plate level and top, respectively. The actual capillary diameter is 10 μm, while the design diameter was 12 μm, which indicates that the voxel width in the lateral direction was about 1 μm. This emitter test structure was written on a single hexagonal chunk whose edges are visible at the right-hand side of the image in the left panel. The high surface quality of the SU-8 structures is obvious from the SEM image. The line extending from the cone at the center to the right results from scan lines starting and ending here. It can be neglected as the defect only affects the surface, with a height/depth in the nanometer range, thus not influencing the structural stability; it nevertheless could be avoided by redesigning the code for this part of the base plate, namely, by having the lines start and end at different, possibly random, angular positions. The SEM image taken from the back side in the right-hand panel of Fig. 4 shows that the diameter at the lower end of the capillary is the same as that at the top and that the capillary surface has the same high quality there; this is where the capabilities of SEM inspection end as far as the capillary is concerned.

The quality and reproducibility of 3D microlithography in SU-8 are also demonstrated by the SEM image in Fig. 5, which depicts a five by five array of volcano emitters with a height of 50 μm above the base plate each, arranged on a square lattice with 40 μm pitch.

Removing unexposed resist from the whole length of the capillary is a well-known challenge even in 3D printing on a larger scale.[18,19] While a continuity check at the end of the fabrication process can confirm that there is a fluidic path through the capillary, the homogeneity of the capillary diameter and quality can only be confirmed by destructive testing. Figure 6 shows the top of a volcano emitter (left panel) and a volcano emitter at the height of the base plate top (right-hand panel), respectively, both milled laterally by a focused ion beam (FIB) to about the center of the capillary.

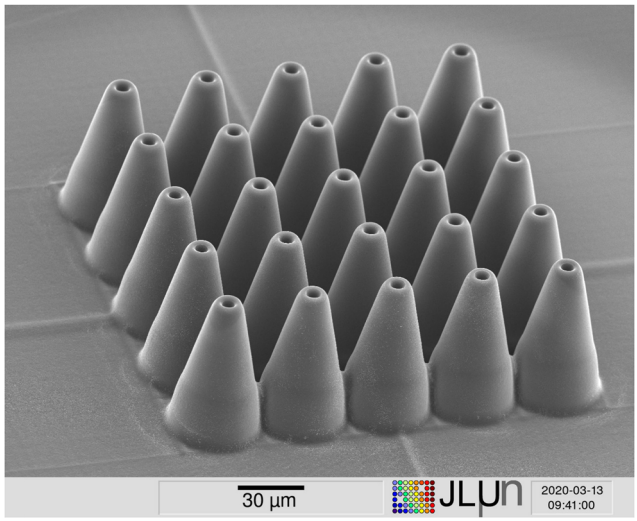

FIG. 5. SEM image of a five by five emitter array.

The FIB inspection shows no signs of incomplete development inside the capillary and suggests that the quality of writing is consistent throughout the entire capillary's length. It is obviously safe to state that capillaries with 10 μm diameter can be reliably fabricated; reducing the diameter further will be the subject of ongoing process optimization.

B. Electric characterization of the emission behavior

Time-resolved current signals from an array of seven microemitters are shown in Fig. 7. The propellant flow rate was kept at a low level, namely, at 0.05 μl min^{-1} for the measurement shown in the top panel and 0.1 μl min^{-1} for the bottom panel, respectively. The data were taken with an oscilloscope (top) and a digital multimeter (bottom). In both cases, the ionic liquid was put at negative

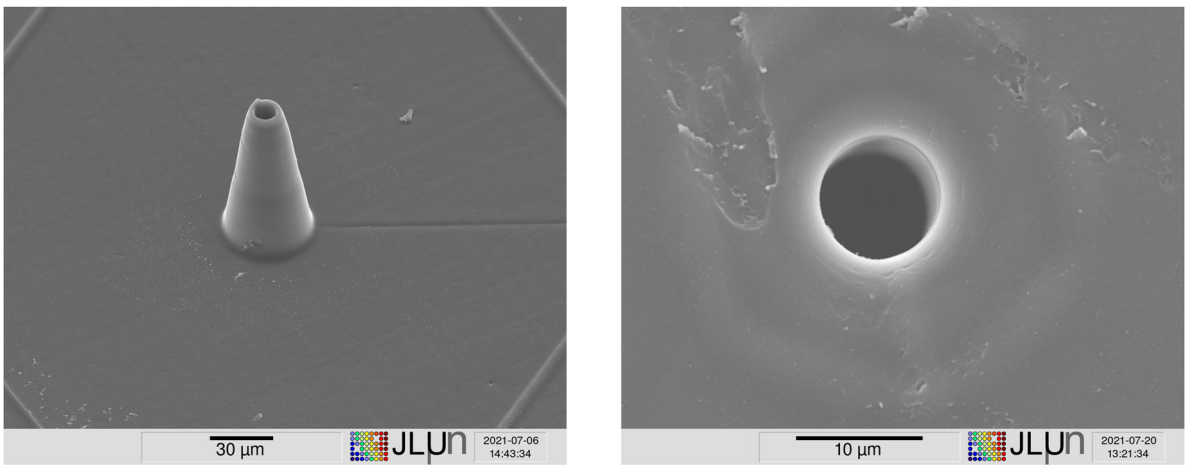

(a) (b)

FIG. 4. SEM images of a single volcano emitter from the (left) top and (right) bottom side.

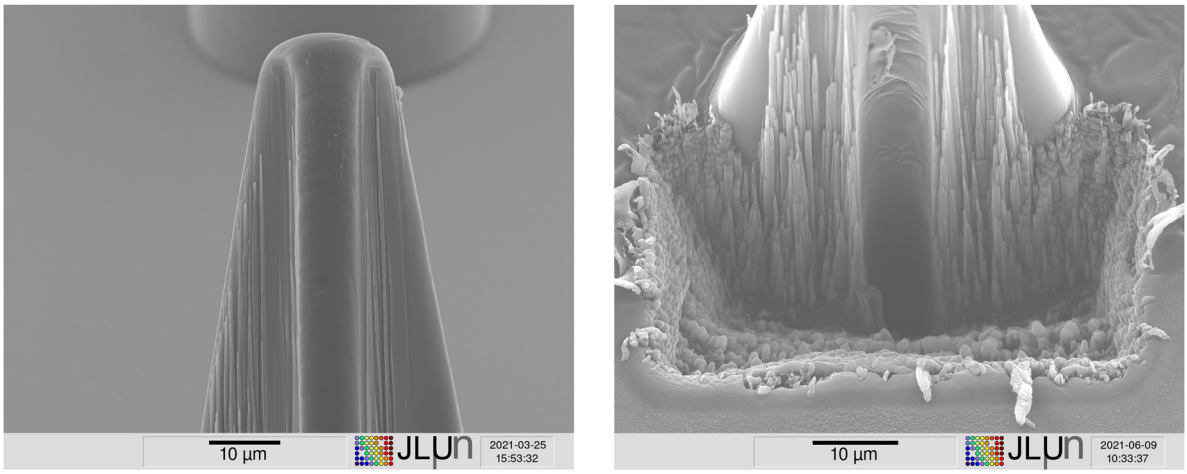

FIG. 6. SEM images of an FIB milled volcano emitter at the tip (left) and at the base plate height (right).

potentials of 2–2.5 kV, and the annular ring extraction electrode with an inner diameter of 1.5 mm and an outer diameter of 3.5 mm was placed at a distance of ~2 mm from the emitters. A caveat at this time is that the geometry of the emission characteristics is not well-known, and it cannot be ruled out that significant portions of the emitted ionic liquid end up on other parts of the (grounded) chamber than the collector plate.

In the low flow regime that data are available for at this time, the emission obviously occurs in the form of single peaks, most likely resulting from rather large droplets that are emitted from one or several of the seven microemitters in the array.

The capillary cross sections realized here with 3D microlithography are more than an order of magnitude lower than those realized by planar and stacked planar photolithography reported earlier by the authors.[11]

Consequently, the currents are comparatively small, and very likely pulsed as there was no stable emission. The experiments revealed that the time resolution of the DC voltmeter (~800 ms) is insufficient to resolve such small pulsed currents. The resolution is primarily limited by the communication with the PC. We were able to resolve such currents on these time scales with the oscilloscope, but it was not possible to record the corresponding data, as the writing speed was too low. Therefore, only single events could be resolved. A ToF setup with improved accuracy is in progress at this time. The new setup features a multi-channel-plate detector, able to resolve even single ion events, with a time resolution in the

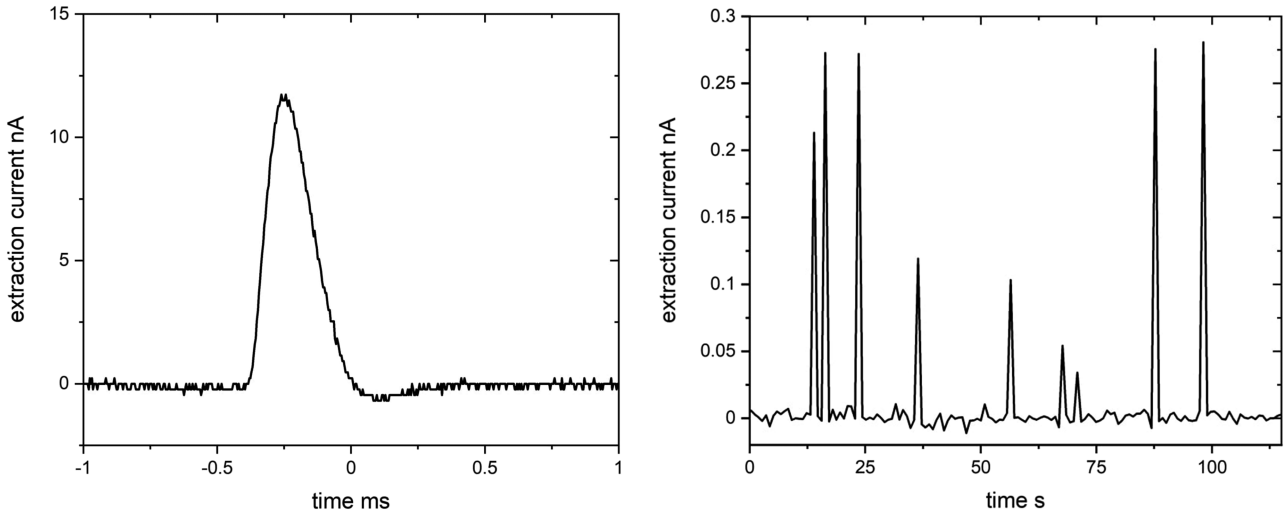

FIG. 7. Extraction current as a function of time for a seven microemitter array: on a short time scale, taken with an oscilloscope (top panel), on a longer time scale, taken with a digital multimeter (bottom panel).

nanosecond range. The detector also features a delay line function giving us access to an axial resolution, revealing the beam spread. Using this new detector, ToF data become available and velocity and mass distributions of the extracted charged species may be determined. We anticipate significant improvement in the beam characterization of our miniaturized emitters using the new equipment.

The emission regimes attainable with the high precision syringe pump controlled flow rate remain to be mapped for the microemitters with 10 μm capillary diameter. In particular, it will be interesting to see how the transition from individual droplets to a continuous emission will be affected by the small capillary diameters, and if individual microemitters arranged in an array indeed are operating independently from each other.

IV. CONCLUSION

The microemitters that are the subject of this report were for the first time made entirely with 3D microlithography, that is, without substrates pre-fabricated with planar photolithography. 3D microlithography is thus proven to be a suitable tool for microemitter fabrication, and the output of more than one finished (ready for measurement) structure per day shows that the Nanoscribe PPGT may even be suitable as a production tool for small series rather than just as a research tool. The overall production cost per unit is lower compared to other fabrication methods, as one unit only requires some readily available photo epoxy, given the necessary infrastructure is available. Furthermore, a rapid prototyping cycle makes this fabrication method rather interesting for commercial and scientific applications.

Currently, there are few other fabrication methods capable of producing emitters of the same quality and size. An example capable of doing so is a silicon-based fabrication method with deep reactive ion etching at its core.[25] Compared to our fabrication method, deep reactive ion etching is incapable of producing undercut profiles and is harshly limited in its freedom of design. Furthermore, this fabrication technique lacks the high resolution of 3D lithography for very small details and has longer production and prototyping cycles.

The newly won design freedom will allow the creation of fluidic structures with increased hydraulic resistance in a well-defined way, which would justify extending the research on miniaturized electrospray emitters to the internally wetted capillary type as an alternative to the successfully established porous emitter type, offering the prospect of further miniaturization by at least one order of magnitude.

The flow regimes across the multiparameter space spanned by flow rate, capillary dimensions, and extraction voltage, to name the most important, need to be mapped both for single emitters and for emitter arrays. Finally, to characterize the composition of the emitted species, an improved ToF setup tailored to the low signal levels needs to be established. Under these circumstances, internally wetted capillary electrospray microemitters still have the potential to become a useful tool in the arsenal of micropropulsion alongside the established porous emitters.

ACKNOWLEDGMENTS

The authors gratefully acknowledge funding by the federal state of Hessen and the European Regional Development Fund (ERDF/EFRE 2014–2 020) (Vorhaben: "Innovationslabor: Physik unter harschen Bedingungen" FKZ: FPG991 0002/2 019). The time-of-flight setup with improved resolution will be funded by the German Federal Ministry for Economic Affairs and Energy under Contract No. (FKZ) 50RS2101.

NOMENCLATURE

The following abbreviations are used in this manuscript:

AOC	attitude and orbit control
DLP	digital light processing
EMIM-BF4	1-ethyl-3-methylimidazolium tetrafluoroborate
FEEP	field emission electric propulsion
FIB	focused ion beam
GWL	NanoScribe specific file format
HVS	high voltage source
IR	infrared
LIS	liquid ion source
PEEK	polyether-ether-ketone
PPGT	type of NanoScribe instrument
SEM	scanning electron microscope or microscopy
SLA	stereo-lithography apparatus

AUTHOR DECLARATIONS

Conflict of Interest

The authors have no conflicts to disclose.

DATA AVAILABILITY

The data that support the findings of this study are openly available in Justus Liebig University's open access data portal JLUpubat at http://dx.doi.org/10.22029/jlupub-117.[27]

REFERENCES

[1] D. R. Lev, G. D. Emsellem, and A. K. Hallock, "The rise of the electric age for satellite propulsion," New Space **5**, 4–14 (2017).
[2] D. Lev, R. M. Myers, K. M. Lemmer, J. Kolbeck, H. Koizumi, and K. Polzin, "The technological and commercial expansion of electric propulsion," Acta Astronaut. **159**, 213–227 (2019).
[3] S. Mazouffre, "Electric propulsion for satellites and spacecraft: Established technologies and novel approaches," Plasma Sources Sci. Technol. **25**, 033002 (2016).
[4] K. Lemmer, "Propulsion for CubeSats," Acta Astronaut. **134**, 231–243 (2017).
[5] K. Holste, P. Dietz, S. Scharmann, K. Keil, T. Henning, D. Zschätzsch, M. Reitemeyer, B. Nauschütt, F. Kiefer, F. Kunze, J. Zorn, C. Heiliger, N. Joshi, U. Probst, R. Thüringer, C. Volkmar, D. Packan, S. Peterschmitt, K.-T. Brinkmann, H.-G. Zaunick, M. H. Thoma, M. Kretschmer, H. J. Leiter, S. Schippers, K. Hannemann, and P. J. Klar, "Ion thrusters for electric propulsion: Scientific issues developing a niche technology into a game changer," Rev. Sci. Instrum. **91**, 061101 (2020).
[6] I. Levchenko, S. Xu, S. Mazouffre, D. Lev, D. Pedrini, D. Goebel, L. Garrigues, F. Taccogna, and K. Bazaka, "Perspectives, frontiers, and new horizons for plasma-based space electric propulsion," Phys. Plasmas **27**, 020601 (2020).
[7] I. Levchenko, S. Xu, Y.-L. Wu, and K. Bazaka, "Hopes and concerns for astronomy of satellite constellations," Nat. Astron. **4**, 1012–1014 (2020).
[8] D. Krejci and P. Lozano, "Space propulsion technology for small spacecraft," Proc. IEEE **106**, 362–378 (2018).

[9]J. Mueller, "Thruster options for microspacecraft—A review and evaluation of existing hardware and emerging technologies," AIAA Paper No. 97-3058, 1997.
[10]G. I. Taylor, "Disintegration of water drops in an electric field," Proc. R. Soc. London, Ser. A **280**, 383–397 (1964).
[11]T. Henning, K. Huhn, and P. J. Klar, "Characterisation of electrospray microemitters fabricated by planar and 3D photolithography," in 36th International Electric Propulsion Conference, IEPC-2019-2344, Vienna, 2019.
[12]B. D. Prince, B. A. Fritz, and Y.-H. Chiu, "Ionic liquids in electrospray propulsion systems," in *Ionic Liquids: Science and Applications* (ACS Publications, 2012), Chap. 2, pp. 27–49.
[13]J. A. Nabity, G. Mason, J. E. Engel, J. W. Daily, R. S. Lagumbay, and D. Kassoy, "Studies of MEMS colloid thrusters," AIAA Paper No. 2006-5007, 2006.
[14]B. S. Peter, R. A. Dressler, Y.-h. Chiu, and T. Fedkiw, "Electrospray propulsion engineering toolkit (ESPET)," Aerospace **7**, 91 (2020).
[15]E. Gustan-Gutierrez and M. Gamero-Castaño, "Microfabricated electrospray thruster array with high hydraulic resistance channels," J. Propul. Power **33**, 984–991 (2017).
[16]D. Courtney, H. Li, P. Lozano, P. GomezMaqueo, and T. Fedkiw, "On the validation of porous nickel as substrate material for electrospray ion propulsion," in *46th AIAA/ASME/SAE/ASEE Joint Propulsion Conference & Exhibit* (AIAA, 2010).
[17]D. Krejci, A. Reissner, B. Seifert, D. Jelem, T. Hörbe, F. Plesescu, P. Friedhoff, and S. Lai, "Demonstration of the IFM nano FEEP thruster in low earth orbit," in 4S Symposium, Sorrento, Italy, 2018.
[18]D. V. M. Máximo and L. F. Velásquez-García, "Additively manufactured electrohydrodynamic ionic liquid pure-ion sources for nanosatellite propulsion," Addit. Manuf. **36**, 101719 (2020).
[19]D. Olvera-Trejo and L. F. Velásquez-García, "Additively manufactured MEMS multiplexed coaxial electrospray sources for high-throughput, uniform generation of core–shell microparticles," Lab Chip **16**, 4121–4132 (2016).
[20]K. Huhn, T. Henning, P. J. Klar, and S. Hengsbach, "Colloid emitters in photostructurable polymer technology: Fabrication and characterization progress report," in 34th International Electric Propulsion Conference, IEPC-2015-120, Kobe, 2015.
[21]K. Huhn, M. Piechotka, T. Henning, and P. J. Klar, "Investigation of the emission behavior of miniaturized SU-8 based colloid emitters," in 33rd International Electric Propulsion Conference, IEPC2013-141, Washington, DC, 2013.
[22]Y.-H. Chiu and R. A. Dressler, *Ionic Liquids for Space Propulsion* (ACS Publications, 2007), pp. 138–160.
[23]R. Martinez-Duarte and M. Madou, *Su-8 Photolithography and its Impact on Microfluidics* (CRC Press, 2011), pp. 231–268.
[24]A. del Campo and C. Greiner, "SU-8: A photoresist for high-aspect-ratio and 3D submicron lithography," J. Micromech. Microeng. **17**, R81–R95 (2007).
[25]S. Dandavino, C. Ataman, C. N. Ryan, S. Chakraborty, D. Courtney, J. P. W. Stark, and H. Shea, "Microfabricated electrospray emitter arrays with integrated extractor and accelerator electrodes for the propulsion of small spacecraft," J. Micromech. Microeng. **24**, 075011 (2014).
[26]J. A. Nabity, "The miniaturization of the colloid thruster to the micro scale," Ph.D. thesis, University of Colorado at Boulder, 2007.
[27]F. L. Kunze, "Data for 'taking internally wetted capillary electrospray emitters to the sub-ten-micrometre scale with 3D microlithography,'" https://doi.org/10.22029/jlupub-117 (2021).